

AERO-THERMO-MECHANICAL CHARACTERISTICS OF FUNCTIONALLY GRADED MATERIAL PANELS WITH TEMPERATURE-DEPENDENT MATERIAL PROPERTIES

Hesham Hamed Ibrahim

Vibration & Acoustic Control Center, Noon for Research and Development, noon.org, Cairo, Egypt,
Hesham.ibrahim@noonrd.org

Mohammad Tawfik

Modeling and Simulation in Mechanics Department, German University in Cairo, Cairo, Egypt,
Mohammad.Tawfik@guc.edu.eg

Mohammed Al-Ajmi

Mechanical Engineering Department, College of Engineering and Petroleum, Kuwait University, P.O. Box 5969,
Safat 13060, Kuwait, malajmi@kuc01.kuniv.edu.kw

ABSTRACT

Background. The concept of functionally graded materials (FGMs) was first introduced as ultrahigh temperature resistant materials for aircrafts. FGMs are non-homogeneous composites characterized by a smooth and continuous change of material properties from one surface to the other. This is achieved by gradually varying the volume fractions of the constituent materials according to certain power law through desired direction(s) in contrast with classical composite materials whose properties vary abruptly from one lamina to the other. FGMs can survive environments with high temperature gradients, while maintaining structural integrity.

Method of Approach. The response of FGM panels will be investigated under the combined effect of elevated temperature conditions and aerodynamic loading using a finite element model based on the thin plate theory and von Karman strain-displacement relations. The aerodynamic pressure is modeled using the quasi-steady first order piston theory. The governing equations are obtained using the principal of virtual work adopting a marching method in temperature to account for temperature dependent material properties. This system of nonlinear equations is solved by Newton-Raphson numerical technique.

Results. The buckling temperature, post buckling deflection, and flutter boundaries are presented under the combined effect of thermal and aerodynamic loadings, illustrating the effect of volume fraction exponent and boundary conditions on the FGM panel response.

Conclusions. It is found that the temperature increase has an adverse effect on the FGM panel flutter characteristics through decreasing the critical dynamic pressure. Decreasing the volume fraction enhances flutter characteristics but this is limited by structural integrity aspect. The presence of aerodynamic flow results in postponing the buckling temperature and in suppressing the post buckling deflection. The clamp boundary condition is found to have better response than the simply supported one.

Keywords: functionally graded material, flutter, thermal buckling

Nomenclature

[A], [B], [D] = in-plane, coupling and bending stiffness matrices of a laminate
[A_a] = aerodynamic stiffness matrix
[G] = aerodynamic damping matrix

h = plate thickness
[K], [M] = system linear stiffness and mass matrices
[K_{tan}] = system tangent stiffness matrix
{N}, {M} = force and moment resultant vectors
 n = volume fraction exponent
[N1], [N2] = system first- and second-order nonlinear stiffness matrices
 Pe = effective material properties of the FGM plate
[Q] = reduced stiffness matrix
 V_c = ceramic volume fraction
{W} = system nodal displacement vector
 u_o, v_o, w_o = initial displacements in x, y and z directions
 α = coefficient of thermal expansion
{ $\Delta\kappa$ } = bending incremental strain vector
 $\Delta\epsilon_m$ = membrane incremental linear strain vector
 $\Delta\epsilon_\theta$ = membrane incremental nonlinear strain vector
 $\Delta\epsilon_o$ = membrane incremental strain vector due to initial deflection
 λ = non-dimensional dynamic pressure

Subscripts

b = bending
 i = iteration number
 m = membrane
 ΔT = due to incremental thermal load
 x, y, z = plate Cartesian coordinates
 w_o = due to initial deflection

1. INTRODUCTION

Panel flutter is a self-excited oscillation of a plate or shell in supersonic flow. Because of aerodynamic pressure forces on the panel, two eigen modes of the structure merge and lead to this dynamic instability. Panel flutter differs from wing flutter only in that the aerodynamic force resulting from the air flow acts only on one side of the panel [1]. Supersonic flutter of plates and shells was recognized to be an important aspect of the design of high speed vehicles when Jordan [2] observed that a number of the early V-2 rocket failures were due to panel flutter. Since then, extensive analytical and experimental research on that subject has been performed. A common remedy to the flutter problem is to stiffen

those panels in danger of flutter, a method that usually introduces additional weight to the design.

Thin plates are a commonly used form of structural component especially in aerospace vehicles, such as high-speed aircraft, rockets, and spacecrafts, which are subjected to thermal loads due to aerodynamic and / or solar radiation heating. This results in a temperature distribution over the surface and thermal gradient through the thickness of the plate. The presence of these thermal fields results in a flutter motion at lower dynamic pressure or a larger limit-cycle amplitude at the same dynamic pressure. In addition, a high temperature rise may cause large thermal deflections (thermal buckling) of the skin panels, which could affect flutter response [3]. Accordingly, it is important to consider the interactive effect of both aforementioned failure characteristics (flutter & buckling). However, it appears that in most past studies, the phenomena of thermal buckling and nonlinear supersonic flutter were investigated separately especially in the field of adaptive and functionally graded materials.

Most flutter analyses can be placed in one of four categories based on the structural and aerodynamic theories employed[4], 1) linear structural theory; quasi-steady aerodynamic theory, 2) linear structural theory; full linearized (inviscid, potential) aerodynamic theory, 3) nonlinear structural theory; quasi-steady aerodynamic theory, 4) nonlinear structural theory; linearized (inviscid, potential) aerodynamic theory. Analyses of the first type have two major weaknesses: a) it does not account for structural nonlinearities, hence it can only determine the flutter boundary and can give no information about the flutter amplitudes, b) the use of quasi-steady aerodynamics neglects the three dimensionality and unsteadiness of the flow, hence it can not be used in the transonic region where the flutter is most likely to occur. Analyses of the second type are intended to remedy weakness b but this type still has weakness a. the third type remedies weakness a but still possesses weakness b. the fourth type remedies both a and b.

A vast amount of literature exists on panel flutter using different aerodynamic theories to model the aerodynamic pressure. The aerodynamic theory employed for the most part of panel flutter at supersonic mach numbers ($M_\infty > 1.4$) is the quasi-steady first order piston theory aerodynamics by Ashley and Zartarian [5]. Mei *et al.* [6] presented a review on the various analytical methods and experimental results of supersonic and hypersonic panel flutter. Liaw [7] studied the geometrically nonlinear supersonic flutter of laminated composite thin plate structures subjected to thermal loads. The formulation based on the classical lamination plate theory. The aerodynamic pressure was modeled using the two-dimensional quasi-steady supersonic theory. Abdel-Motagaly *et al.* [8] investigated the effect of arbitrary flow direction on the large amplitude supersonic flutter of composite panels, using the von Karman strain-displacement relation to account for large amplitude limit-cycle oscillations. Mei [9] developed a finite element approach for determining nonlinear flutter characteristics of two dimensional panels, based on aerodynamic forces from quasi-steady aerodynamic theory. Dixon and Mei [10] presented a nonlinear flutter analysis of thin composite panels using finite element method. The governing equation of motion was formulated using the principle of virtual work, while the eigen value problem was solved by utilizing the linearized updated mode with nonlinear time function (LUM/NTF) approximation. Sarma and Varadan [11] studied the nonlinear flutter by using the finite element method. The governing equations were derived from energy considerations using Lagrange's equations of motion without any approximation on nonlinear terms pertaining to

moderately large oscillations. Xue and Mei [1] presented an innovative finite element frequency domain solution for the nonlinear flutter response of panels under the combined effect of thermal and aerodynamic loads. Dongi [12] investigated the nonlinear flutter of flat and slightly curved panels in high supersonic flow based on von Karman plate model and on the linear piston theory for aerodynamics. Lee *et al.* [13] performed the thermal post buckling and aerodynamic-thermal load analysis of cylindrical laminated panels using the finite element method. The panel flutter analysis under thermal stresses was carried out using Hans Krumhaar's supersonic piston theory to model aerodynamic pressure.

Extensive research work has been carried out on the FGM since its concept was proposed in the late 1980s in Japan. FGMs are non-homogeneous composites characterized by a smooth and continuous change of material properties from one surface to the other. This is achieved by gradually varying the volume fraction of the constituent materials. One of the advantages of using these materials is that they can survive environments with high temperature gradients, while maintaining structural integrity. Functionally graded materials are usually composed of two or more materials whose volume fractions are changing smoothly and continuously along desired direction(s). This continuous change in the compositions leads to a smooth change in the mechanical properties, which has many advantages over the laminated composites, where the delamination and cracks are most likely to initiate at the interfaces due to the abrupt variation in the mechanical properties between laminas [14].

Dai *et al.* [14] presented a mesh free model for the active shape control and the dynamic response suppression of a functionally graded material plate containing piezoelectric sensors and actuators. Birman [15] studied the stability of functionally graded shape memory alloy (SMA) hybrid sandwich panels under the simultaneous action of in-plane compressive and thermal loadings. Functional grading was achieved by a nonuniform distribution of shape memory alloy fibers in the middle plane (sinusoidal distribution). El-Abbassi and Meguid [16] presented a new thick shallow shell element to study the thermoelastic behavior of functionally graded structures made from shells and plates. The element accounts for the varying elastic and thermal properties across its thickness. Reddy [17] presented theoretical formulation, Navier's solutions of rectangular plates, and finite element model based on the third order shear deformation plate theory for the analysis of through the thickness functionally graded plates. The formulation accounts for the thermo-mechanical coupling, time dependency, and von Karman-type geometric nonlinearity. He *et al.* [18] presented a finite element formulation based on the classical laminated plate theory for the shape and vibration control of functionally graded material plates with integrated piezoelectric sensors and actuators. A constant velocity feedback control algorithm was used for the active control of the dynamic response of the FGM plate through closed loop control. Javaheri and Eslami [19] derived the equilibrium and stability equations of a rectangular plate made of a functionally graded material under thermal loads adopting the higher order shear deformation plate theory. A buckling analysis of a functionally graded plate under four types of thermal loads is carried out and a closed form solution for the prediction of the buckling temperature for rectangular simply supported FGM plate was obtained. Woo *et al.* [20] developed an analytical solution for the post buckling behavior of plates and shallow cylindrical shells made of functionally graded materials under the simultaneous action of

compressive in-plane loads and a temperature field. The solution is obtained in terms of mixed Fourier series. Yang *et al.* [21] investigated the geometrically non-linear bending behavior of functionally graded plates with integrated piezoelectric layers and subjected to transverse loads and a temperature gradient through the plate thickness. Reddy's higher-order shear deformation plate theory was adopted. Zenkour [22] studied the static response for a simply supported functionally graded rectangular plate subjected to a transverse uniform load using a generalized shear deformation theory. The effect of transverse shear deformation, plate aspect ratio, side-to-thickness ratio, and volume fraction distributions were presented. It is found from the analysis that the response of a FGM plate is intermediate to that of the ceramic and metal homogeneous plates. Kim [23] developed an analytical technique to investigate the effect of temperature on the vibration characteristics of thick functionally graded rectangular plates, taking into account the temperature dependence of the material properties. Batra and Jin [24] adopted the first-order shear deformation theory (FSDT) coupled with finite element method to study the vibration of functionally graded anisotropic rectangular plate with different edge support conditions. The grading here is achieved through continuously changing the fiber orientation angle through the thickness. Qian and Batra [25] adopted the meshless local Petrov-galerkin (MLPG) method and the compatible higher order shear and normal deformation plate theory (HOSNDPT) to a thick two constituent functionally graded cantilever plate. The volume fractions of the constituents are assumed to vary in x- and y-directions. The spatial volume fractions of the constituents are optimized so as to maximize either the first or the second natural frequency of the plate. Tauchart [26] presented a comprehensive literature review on thermally induced flexure, buckling, and vibration of plates. Consideration was given to thin and moderately thick plates, plates having various support conditions, and isotropic as well as anisotropic or heterogeneous material behaviors. Gray and Mei [27] investigated the thermal post-buckling behavior and free vibrations of thermally buckled composite plates using the finite element method. Thornton [28] presented a comprehensive review on the thermal buckling of plates and shells demonstrating thermal buckling and post-buckling research for plates, shallow shells and curved panels, cylindrical and conical shells. Parkash and Ganapathi [29] adopted the finite element method to investigate the supersonic flutter behavior of flat panels made of functionally graded material under the influence of thermal environment. Temperature dependent material properties were only assumed while calculating material properties through the thickness, but not while increasing the temperature to reach buckling.

In this work, the flutter and post-buckling behavior of a ceramic-metal functionally graded plate under thermal and aerodynamic loadings are studied using nonlinear finite element method. The nonlinear governing equations for thin rectangular functionally graded plate are obtained using the principle of virtual work and the von Karman strain-displacement relation. An incremental method is presented which is capable of handling the problem of temperature dependent material properties. Numerical results are provided to show the effect of thermal field, material properties, volume fraction exponent and boundary conditions on the post buckling and critical dynamic pressure of functionally graded rectangular plates.

2. Finite Element Formulation of Thermal Post-Buckling Of FGM Panels

The equation of motion with the consideration of large deflection and temperature dependent (TD) material properties are derived for a functionally graded plate subject to aerodynamic and thermal loadings. To account for temperature dependency of material properties, a marching method in temperature is adopted for the calculation of the thermal deflection and stresses in the plate. The element used in this study is the rectangular four-node-Bogner-Fox-Schmidt (BFC) C^1 conforming element (for the bending DOFs).

2.1. The Displacement-Nodal Displacement Relation

The degrees of freedom vector of the rectangular plate element can be written

$$\{\delta\} = \left\{ w, \frac{\partial w}{\partial x}, \frac{\partial w}{\partial y}, \frac{\partial^2 w}{\partial x \partial y}, u, v \right\}^T = \begin{Bmatrix} w_b \\ w_m \end{Bmatrix} \quad (1)$$

where $\{w_b\}$ is the transverse displacement vector and $\{w_m\}$ is the membrane displacement vector. The displacement-nodal displacement relation can be presented in terms of interpolation function matrices, $[N_w]$, $[N_u]$ and $[N_v]$ as:

$$w = [N_w] \{w_b\}^e, \quad u = [N_u] \{u\}^e \quad (2)$$

and $v = [N_v] \{v\}^e$

where the superscript, e, indicates element degrees of freedom.

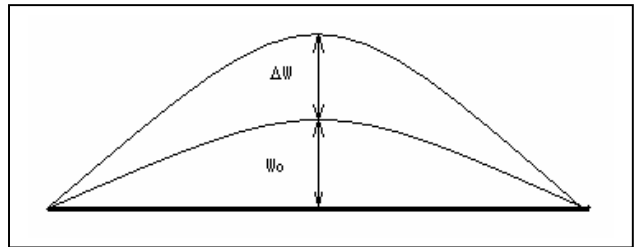


Figure 1 Lateral deflection diagram of panel

2.2. The Nonlinear Strain-Displacement Relation

An incremental method is derived, to account for the temperature dependent material properties, for the calculation of the thermal deflections and stresses in the FGM panel. Consider the lateral deflection sketch shown in Figure 1) [3] utilizing the incremental method and the von Karman large deflection strain-displacement relation; the incremental strain-displacement relation can be written as:

$$\begin{Bmatrix} \Delta \varepsilon_x \\ \Delta \varepsilon_y \\ \Delta \gamma_{xy} \end{Bmatrix} = \begin{Bmatrix} \frac{\partial \Delta u}{\partial x} \\ \frac{\partial \Delta v}{\partial y} \\ \frac{\partial \Delta u}{\partial y} + \frac{\partial \Delta v}{\partial x} \end{Bmatrix} + \begin{Bmatrix} \frac{1}{2} \left(\frac{\partial \Delta w}{\partial x} \right)^2 \\ \frac{1}{2} \left(\frac{\partial \Delta w}{\partial y} \right)^2 \\ \frac{\partial \Delta w}{\partial x} \frac{\partial \Delta w}{\partial y} \end{Bmatrix} \quad (3)$$

$$+ \begin{Bmatrix} \frac{\partial \Delta w}{\partial x} \frac{\partial w_o}{\partial x} \\ \frac{\partial \Delta w}{\partial y} \frac{\partial w_o}{\partial y} \\ \frac{\partial \Delta w}{\partial x} \frac{\partial w_o}{\partial y} + \frac{\partial \Delta w}{\partial y} \frac{\partial w_o}{\partial x} \end{Bmatrix} + z \begin{Bmatrix} -\frac{\partial^2 \Delta w}{\partial x^2} \\ -\frac{\partial^2 \Delta w}{\partial y^2} \\ -2 \frac{\partial^2 \Delta w}{\partial x \partial y} \end{Bmatrix}$$

or in compact form

$$\{\Delta \varepsilon\} = \{\Delta \varepsilon_m\} + \{\Delta \varepsilon_\theta\} + \{\Delta \varepsilon_o\} + z \{\Delta \kappa\} \quad (4)$$

where Δw , shown in Figure 1), denotes the incremental transverse displacement. Parameters u_o , v_o and w_o are initial displacements in x , y and z directions, respectively. $\Delta \varepsilon_m$, $\Delta \varepsilon_\theta$, $\Delta \varepsilon_o$ and $z \Delta \kappa$ are the membrane incremental linear strain vector, the membrane incremental nonlinear strain vector, the membrane incremental strain vector due to initial deflection and the bending incremental strain vector, respectively.

2.3. Functionally Graded Materials

Typically, the FGMs are made of a mixture of two materials; a ceramic, which is capable of withstanding high temperature environments due to its low thermal conductivity and a metal which act as a structural element to support loading and prevent fractures. Without losing generality, it is usually assumed that the top surface of an FGM plate is ceramic rich and the bottom is metal rich. The region between the two surfaces consists of a blend of the two materials which is assumed in the form of a simple power law distribution as [14]:

$$P_e(z) = P_C V_C + P_M (1 - V_C) \quad (5)$$

$$V_C = \left(0.5 + \frac{z}{h} \right)^n, \quad (-h/2 \leq z \leq h/2, 0 \leq n \leq \infty) \quad (6)$$

where z is coordinate in the thickness direction of a plate; (P_e , P_C , P_M) are effective material properties of the FGM, the properties of the ceramic and the properties of the metal respectively, V_C is the ceramic volume fraction and h is the plate thickness. Power n is the volume fraction exponent.

Figure (2) shows the variation of the volume fraction function versus non-dimensional thickness with different volume fraction exponent n . Functional grading could be also achieved through smoothly changing the fiber orientation of a composite laminate through the plate thickness, or through a nonuniform distribution of the fibers in the plane of the plate [15].

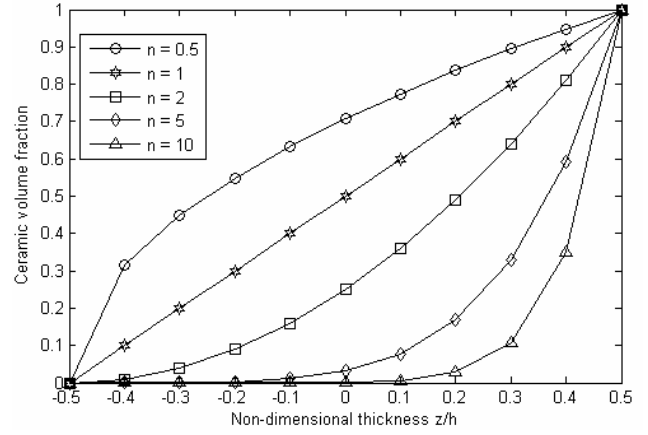


Figure 2 Variation of the ceramic volume fraction function versus the non-dimensional thickness z/h

2.4. Stress-Strain Relationship of an FGM Panel

The relationship of inplane forces $\{N\}$ and bending moments $\{M\}$ in terms of the strain vector can be written as [3]:

$$\begin{Bmatrix} N \\ M \end{Bmatrix} = \begin{Bmatrix} N_o \\ M_o \end{Bmatrix} = \begin{bmatrix} A & B \\ B & D \end{bmatrix} \begin{Bmatrix} \varepsilon \\ \kappa \end{Bmatrix} - \begin{bmatrix} A_o & B_o \\ B_o & D_o \end{bmatrix} \begin{Bmatrix} \varepsilon_o \\ \kappa_o \end{Bmatrix} \quad (7)$$

$$- \begin{Bmatrix} N_T \\ M_T \end{Bmatrix} = \begin{Bmatrix} N_{T_o} \\ M_{T_o} \end{Bmatrix}$$

where

$$(A, B, D) = \int_{-h/2}^{h/2} (1, Z, Z^2) [Q(Z)] dZ$$

$$Q(z) = \begin{bmatrix} \frac{E(z)}{1 - \nu^2(z)} & \frac{\nu E(z)}{1 - \nu^2(z)} & 0 \\ \frac{\nu E(z)}{1 - \nu^2(z)} & \frac{E(z)}{1 - \nu^2(z)} & 0 \\ 0 & 0 & \frac{E(z)}{2(1 + \nu(z))} \end{bmatrix}$$

where $[A]$, $[B]$ and $[D]$ are the extensional matrix, extensional-bending coupling matrix and flexural matrix, respectively. The subscripts o and T denote initial value and thermal. Assuming constant temperature distribution in the x , y and z directions, and that the temperature-dependent properties are constant in the increment $\Delta T = T - T_o$ with the values set to that of temperature T , equation (7) can be rewritten as follows:

$$\begin{Bmatrix} N \\ M \end{Bmatrix} = \begin{bmatrix} A & B \\ B & D \end{bmatrix} \begin{Bmatrix} \Delta \varepsilon \\ \Delta \kappa \end{Bmatrix} - \begin{Bmatrix} N_{\Delta T} \\ M_{\Delta T} \end{Bmatrix} + \begin{Bmatrix} N_o \\ M_o \end{Bmatrix} \quad (8)$$

Substituting equation (4) into (8) yields

$$\{N\} = [A]\{\Delta\varepsilon_m + \Delta\varepsilon_\theta + \Delta\varepsilon_o\} + [B]\{\Delta\kappa\} - \{N_{\Delta T}\} + \{N_o\} \quad (9)$$

$$\{M\} = [B]\{\Delta\varepsilon_m + \Delta\varepsilon_\theta + \Delta\varepsilon_o\} + [D]\{\Delta\kappa\} - \{M_{\Delta T}\} + \{M_o\} \quad (10)$$

2.5. Governing Equation of the Thermal Post-Buckling Deflection

Using the principle of virtual work and equations (2), (4), (9) and (10), the governing equation of thermal post-buckling deflection can be obtained in terms of incremental transverse deflection, $\{\Delta W_b\}$, and incremental inplane deflection, $\{\Delta W_m\}$.

$$\left(\begin{array}{c} \left[\begin{array}{cc} [K_b] & [K_{bm}] \\ [K_{mb}] & [K_m] \end{array} \right] - \left[\begin{array}{cc} [K_{N\Delta T b}] & 0 \\ 0 & 0 \end{array} \right] + \left[\begin{array}{cc} [K_{ob}] & 0 \\ 0 & 0 \end{array} \right] \\ + \left[\begin{array}{cc} [K1_{womb}] + [K2_{wob}] & [K1_{wobm}] \\ [K1_{womb}] & 0 \end{array} \right] \\ + \frac{1}{2} \left[\begin{array}{cc} [N1_{womb}] & 0 \\ 0 & 0 \end{array} \right] \\ + \frac{1}{2} \left[\begin{array}{cc} [N1_{nmb}] + [N1_{nb}] & [N1_{bm}] \\ [N1_{mb}] & 0 \end{array} \right] \\ + \frac{1}{3} \left[\begin{array}{cc} [N2_{wb}] & 0 \\ 0 & 0 \end{array} \right] \end{array} \right) \left\{ \begin{array}{c} \{\Delta W_b\} \\ \{\Delta W_m\} \end{array} \right\} \quad (11)$$

$$= \left\{ \begin{array}{c} \{P_{b\Delta T}\} \\ \{P_{m\Delta T}\} \end{array} \right\} - \left\{ \begin{array}{c} \{P_{bo}\} \\ \{P_{mo}\} \end{array} \right\} + \left\{ \begin{array}{c} \{P_{wob\Delta T}\} \\ 0 \end{array} \right\} - \left\{ \begin{array}{c} \{P_{owob}\} \\ 0 \end{array} \right\}$$

Equation (11) can be rewritten in compact form as:

$$\left(\begin{array}{c} [K] - [K_{N\Delta T}] + [K_o] + [K_{wo}] + \frac{1}{2}[N1_{wo}] \\ + \frac{1}{2}[N1] + \frac{1}{3}[N2] \end{array} \right) \{\Delta W\} \quad (12)$$

$$= \{P_{\Delta T}\} - \{P_o\} + \{P_{wob\Delta T}\} - \{P_{owob}\}$$

where $[K]$, $[K_{N\Delta T}]$, $[K_o]$ and $[K_{wo}]$ denote the linear stiffness matrix, the incremental thermal geometric stiffness matrix, the initial stress geometric stiffness matrix and the initial deflection linear stiffness matrix, respectively. $[N1_{wo}]$ is a stiffness term that depends on the initial deflection and is a first-order nonlinear term in the incremental deflection; $[N1]$ and $[N2]$ are the first-order nonlinear incremental stiffness matrix and the second order nonlinear incremental stiffness matrix, respectively. $\{P_{\Delta T}\}$, $\{P_o\}$, $\{P_{wob\Delta T}\}$ and $\{P_{owob}\}$ indicate the incremental thermal load vector, the initial stress load vector, the incremental thermal load vector due to initial deflections and the load vector due to initial load and initial deflections, respectively[3].

3. Solution Procedures and Results of Thermal Post-Buckling of FGM Plates

In this section, the solution procedure for predicting the thermal post-buckling behavior of FGM plates is presented. Then,

the effect of the volume fraction exponent, n , and the boundary conditions on the buckling temperature and post-buckling deflection will be demonstrated.

3.1. The Post-Buckling Deflection Problem

Introducing the function $\{\Psi(W)\}$ to the equation (12),

$$\{\Psi(\Delta W)\} = \left(\begin{array}{c} [K] - [K_{N\Delta T}] + [K_o] + [K_{wo}] + \frac{1}{2}[N1_{wo}] \\ + \frac{1}{2}[N1] + \frac{1}{3}[N2] \end{array} \right) \{\Delta W\} \quad (13)$$

$$- \{P_{\Delta T}\} + \{P_o\} - \{P_{wob\Delta T}\} + \{P_{owob}\} = 0$$

This can be written using truncated Taylor expansion as follows:

$$\{\Psi(\Delta W + \delta W)\} = \{\Psi(\Delta W)\} + \frac{d\{\Psi(\Delta W)\}}{d(\Delta W)} \{\delta W\} = 0 \quad (14)$$

where

$$\frac{d\{\Psi(\Delta W)\}}{d(\Delta W)} = \left(\begin{array}{c} [K] - [K_{N\Delta T}] + [K_o] + [K_{wo}] + [N1_{wo}] \\ + [N1] + [N2] \end{array} \right) \quad (15)$$

$$= [K_{tan}]$$

thus, the Newton-Raphson iterative procedures for the determination of the post buckling deflection can be expressed as follows:

$$\{\Psi(\Delta W)\}_i = \left(\begin{array}{c} [K] - [K_{N\Delta T}] + [K_o] + [K_{wo}] + \frac{1}{2}[N1_{wo}] \\ + \frac{1}{2}[N1] + \frac{1}{3}[N2] \end{array} \right) \{\Delta W\} \quad (16)$$

$$- \{P_{\Delta T}\} + \{P_o\} - \{P_{wob\Delta T}\} + \{P_{owob}\}$$

$$[K_{tan}]_i \{\delta W\}_{i+1} = -\{\Psi(\Delta W)\}_i \quad (17)$$

$$\{\delta W\}_{i+1} = -[K_{tan}]_i^{-1} \{\Psi(\Delta W)\}_i \quad (18)$$

$$\{\Delta W\}_{i+1} = \{\Delta W\}_i + \{\delta W\}_{i+1} \quad (19)$$

Convergence occurs in the above procedure when the maximum value of $\{\delta W\}_{i+1}$ becomes less than a given tolerance ε_{tol} ; i.e. $\max |\{\delta W\}_{i+1}| \leq \varepsilon_{tol}$.

3.2. Numerical Simulation of Buckling and Post-Buckling Suppression of an FGM Panel

In this section, thermal buckling and post-buckling analysis are carried out for an FGM panel which is a mixture of nickel and silicon nitride (Si_3N_4) to figure out the effect the volume fraction exponent, n , and the different boundary conditions on the buckling characteristics of the FGM panel. The material properties are assumed to be temperature dependent according to the following relation [29]:

$$P = P_o(P_{-1}T^{-1} + 1 + P_1T + P_2T^2 + P_3T^3) \quad (20)$$

The coefficients P_o , P_{-1} , P_1 , P_2 and P_3 for young's modulus E , the Poisson ratio ν and the thermal expansion coefficient α of nickel and silicon nitride are given in Table (1). The geometry of the panel is chosen to be $0.305 \times 0.305 \times 0.002\text{m}$. A 6×6 mesh is adopted in this simulation, as solution convergence is found to occur at this mesh size.

Table 1 Temperature-dependence coefficients for silicon nitride and nickel[29]

Properties	Material	P_{-1}	P_o	P_1	P_2	P_3
E (MPa)	Si ₃ N ₄	0	348.43e9	-3.07e-4	2.2e-7	-8.9e-11
	Nickel	0	223.95e9	-2.79e-4	3.9e-9	0
ν	Si ₃ N ₄	0	0.24	0	0	0
	Nickel	0	0.31	0	0	0
α	Si ₃ N ₄	0	5.8723e-6	9.09e-4	0	0
	Nickel	0	9.9209e-6	8.71e-4	0	0
ρ (Kg/m ³)	Si ₃ N ₄	2370				
	Nickel	8900				

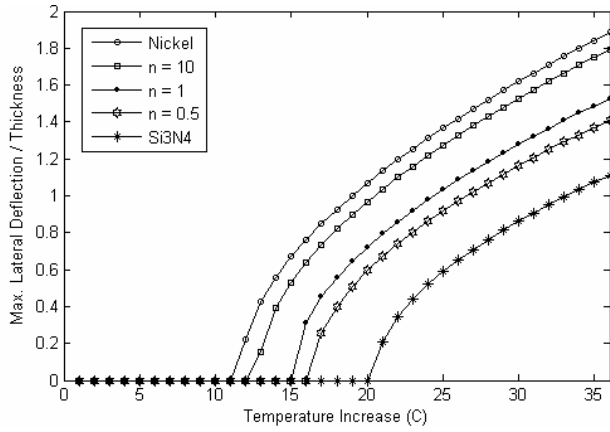


Figure 3 Post-Buckling deflection for a clamped FGM panel with different volume fraction exponent n

Figure (3) illustrates the effect of the volume fraction exponent on the buckling characteristics of a clamped FGM panel. The results of the buckling temperatures seen in the figure were found to be in a good agreement with those calculated by Javaheri and Eslami [19]. It is seen that the responses that corresponds to properties intermediate to that of the metal and the ceramic lie between that of the metal and ceramic, and this consistent with what is mentioned by Reddy [17].

It is seen in figure (4) that for functionally graded material panels with simply supported edges, there is no buckling phenomena because any small temperature rise results in a prompt transverse deflection of the panel due to structural asymmetry about the middle plane of the FGM panel that makes all simply supported FGM panels lose their buckling phenomena.

Although, the ceramic panel response seems to be superior to that of the FGM panel, but using the ceramic panel results in a structural integrity problem due to the brittleness of the ceramic. So, it is worth while noting that increasing the ceramic volume fraction is bounded by structural integrity aspects.

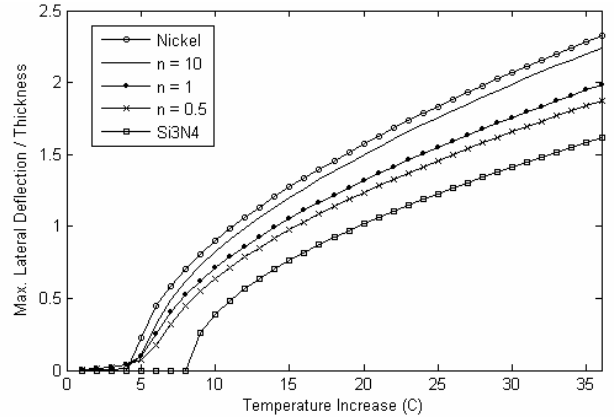


Figure 4 Post-Buckling deflection for a simply supported FGM panel with different volume fraction exponent n

4. Finite Element Formulation of Panel-Flutter under Thermal Effect

In this section, the formulation will be extended to include the dynamic terms to study the panel-flutter problem of FGM panels under the effect of thermal loading. The aerodynamic loading is modeled using the first-order quasi-steady piston theory which gives quite an accurate aerodynamic model at mach numbers greater than $\sqrt{2}$ [6].

4.1. Derivation of the Element Matrices for the Combined Loading Problem

The first-order quasi-steady piston theory for supersonic flow states that [3]:

$$P_a = -\frac{2q}{\beta} \left[\left(\frac{M_\infty - 2}{M_\infty - 1} \right) \frac{1}{v} \frac{\partial w}{\partial t} + \frac{\partial w}{\partial x} \right] \quad (21)$$

$$= -\left(\frac{g_a}{\omega_o} \frac{D_{110}}{a^4} \frac{\partial w}{\partial t} + \lambda \frac{D_{110}}{a^3} \frac{\partial w}{\partial x} \right)$$

With

$$q = \frac{\rho_a v^2}{2}, \quad \beta = \sqrt{M_\infty^2 - 1}, \quad \omega_o = \left(\frac{D_{110}}{\rho h a^4} \right)^{\frac{1}{2}},$$

$$g_a = \frac{\rho_a v (M_\infty^2 - 2)}{\rho h \omega_o \beta^3} \quad \text{and} \quad \lambda = \frac{2q a^3}{\beta D_{110}}$$

Where P_a is the aerodynamic loading, v is the velocity of airflow, M_∞ is the Mach number, q is the dynamic pressure, ρ_a is the air mass density, g_a is non-dimensional aerodynamic damping, λ is non-dimensional aerodynamic pressure, D_{110} is the first entry of the flexural stiffness matrix $D(1, 1)$ and a is the panel length.

The virtual work of aerodynamic loading, P_a , using the quasi-steady first-order piston theory can be written as:

$$\int_A \delta w P_a dA = - \int_A \delta w \left(\frac{g_a}{\omega_o} \frac{D_{110}}{a^4} \frac{\partial w}{\partial t} + \lambda \frac{D_{110}}{a^3} \frac{\partial w}{\partial x} \right) dA \quad (22)$$

$$= - \{\delta w_b\}^T \frac{g_a}{\omega_o} [g] \{\dot{w}_b\} - \{\delta w_b\}^T \frac{\lambda}{a^3} [a_a] \{w_b\}$$

where $[g]$ is the aerodynamic damping matrix and $[a_a]$ is the aerodynamic influence (stiffness) matrix. Including the dynamic and aerodynamic terms in the equation of motion and reducing the model for the linear solution of an FGM panel subject to uniform temperature distribution, by dropping all the terms that depend on the dynamic deflection (W_b), the equation becomes:

$$\begin{bmatrix} [M_b] & 0 \\ 0 & [M_m] \end{bmatrix} \begin{Bmatrix} \ddot{W}_b \\ \ddot{W}_m \end{Bmatrix} + \frac{g_a}{\omega_o} \begin{bmatrix} [G] & 0 \\ 0 & 0 \end{bmatrix} \begin{Bmatrix} \dot{W}_b \\ \dot{W}_m \end{Bmatrix} + \begin{bmatrix} [K_b] - [K_{N\Delta T}] + \frac{\lambda}{a^3} [A_a] + \frac{1}{2} [N1_{nmb}] & [K_{bm}] \\ [K_{mb}] & [K_m] \end{bmatrix} \begin{Bmatrix} W_b \\ W_m \end{Bmatrix} = 0 \quad (23)$$

It can be assumed that the inplane mass term $[M_m]$ is negligible, thus, according to equation (23), inplane dynamic deflection $\{W_m\}$ can be expressed as:

Equation (23) can be represented in terms of $[W_b]$,

$$\begin{bmatrix} [M_b] \end{bmatrix} \ddot{W}_b + \frac{g_a}{\omega_o} [G] \dot{W}_b + \begin{bmatrix} [K_b] - [K_{N\Delta T}] + \frac{1}{2} [N1_{nmb}] \\ + \frac{\lambda}{a^3} [A_a] - [K_{bm}] [K_m]^{-1} [K_{mb}] \end{bmatrix} W_b = 0 \quad (24)$$

Note that, in equation (24), the term $[N1_{nmb}]$ is evaluated using the value of $\{\Delta W_m\}$ evaluated at the static analysis of this temperature step. We assume the deflection function of the transverse displacement $\{W_b\}$ to be in the form of

$$\{W_b\} = \bar{c} \{\Phi_b\} e^{\Omega t} \quad (25)$$

Where $\Omega = \alpha + i\omega$ is the complex panel motion parameter (α is the damping ratio and ω is the frequency), \bar{c} is the amplitude of vibration, and $\{\Phi_b\}$ is the mode shape.

Substituting equation (25) into (24), the generalized eigenvalue problem can be obtained as

$$\bar{c} \left[-\kappa [\bar{M}_b] + [K] \right] \{\Phi_b\} e^{\Omega t} = \{0\} \quad (26)$$

Where $[\bar{M}_b] = \omega_o^2 [M_b]$, κ is the non-dimensional eigenvalue, given by

$$\kappa = - \left(\frac{\Omega^2}{\omega_o^2} \right) - \frac{g_a \Omega}{\omega_o} \quad (27)$$

and

$$\begin{aligned} [\bar{K}] &= [K_b] - [K_{N\Delta T}] + \frac{1}{2} [N1_{nmb}] + \frac{\lambda}{a^3} [A_a] \\ &\quad - [K_{bm}] [K_m]^{-1} [K_{mb}] \end{aligned} \quad (28)$$

From equation (26) we can write the generalized eigenvalue problem,

$$\left[-\kappa [\bar{M}_b] + [\bar{K}] \right] \{\Phi_b\} = \{0\} \quad (29)$$

where κ is the eigenvalue, and Φ_b is the mode shape, with the characteristic equation written as,

$$\left| -\kappa [\bar{M}_b] + [\bar{K}] \right| = \{0\} \quad (30)$$

Given that the values of κ are real for all values of λ below the critical value, an iterative solution can be utilized to determine the critical non-dimensional dynamic pressure λ_{cr} .

The aerodynamic stiffness term ($(\lambda/a^3) [A_a]$) can be added to the procedure of section (3) to investigate the effect of changing the dynamic pressure on the buckling and post buckling deflection of an FGM panel.

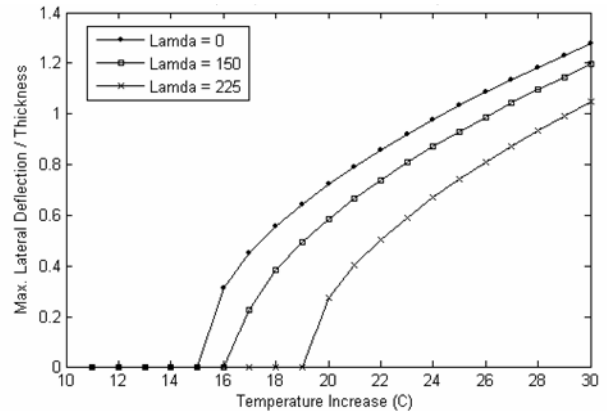


Figure 5 the effect of the different values of the dynamic pressure on the buckling characteristics of an FGM panel

Figure (6) illustrates the effect of changing the value of the dynamic pressure on the buckling temperature and post-buckling deflection of a nickel-silicon nitride FGM clamped panel with the volume fraction exponent n equals one ($n=1$). It seen clearly that the presence of the air flow increases the stiffness of the panel.

4.2. Numerical results for predicting the stability boundaries of an FGM panel

In this section, the stability boundaries of an FGM panel with clamped edges and with different Volume fraction exponent, n will be studied. The results of the combined loading stability boundaries were obtained by two different methods. To obtain the flutter boundary, the dynamic pressure is increased at a certain temperature until the coalescence of two eigen modes, i.e. until

flutter occurs. To have the thermal buckling boundary, the critical buckling temperature is calculated with dynamic pressure as a parameter.

An FGM panel under the effect of thermal and aerodynamic loading is presented in figure (5) in terms of the critical temperature boundary and linear flutter boundary. The area of the graph is divided into three regions; the flat panel region, in which the panel is stable, i.e. neither buckling nor panel flutter, occurred; the buckled region, in which the thermal stresses overcome the panel stiffness and aerodynamic stiffness. In this region, the panel undergoes static instability under inplane thermal loading; the third region is the flutter region, where the panel undergoes dynamic instability under the influence of aerodynamic pressure. Thus, the wider the flat panel region is, the more stable the panel is. It seen in figure (5) that decreasing the volume fraction exponent n , results in a wider flat panel region and in turn a more stable panel.

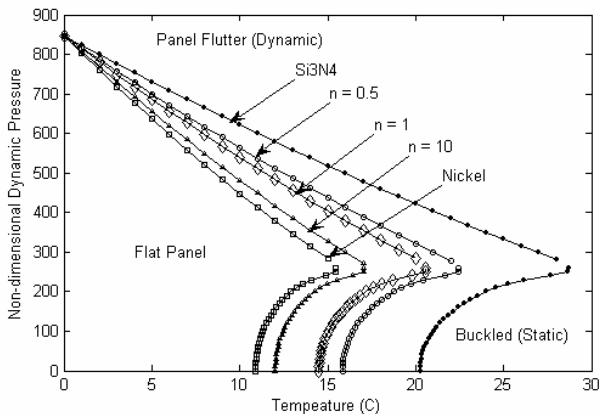


Figure 6 the effectiveness of the volume fraction exponent n on the stability boundaries of an FGM clamped panel

5. Conclusions

An efficient finite element formulation was presented for the analysis of supersonic panel flutter and buckling characteristics of an FGM panel made of nickel and silicon nitride. Nonlinear temperature-dependent material properties and von Karman large deflection was considered in the formulation. The material properties were assumed to vary through the thickness direction based on a simple power law distribution. The aerodynamic forces were modeled using the quasi-steady first-order piston theory. An incremental method in temperature was adopted to take into account the temperature dependency of material properties.

The effectiveness of the volume fraction exponent and the boundary conditions on the linear flutter and the buckling characteristics of the FGM panel were studied. The results showed that the presence of the silicon nitride with the nickel enhances the buckling characteristics of the panel through increasing the buckling temperature and decreasing the post-buckling deflection.

Functionally graded material panels with simply supported edges has no buckling phenomena because any small temperature rise results in a prompt transverse deflection of the panel due to structural asymmetry about the middle plane. For a given temperature, it was also found that decreasing the volume fraction exponent enhances flutter characteristics through increasing the

critical dynamic pressure. The presence of aerodynamic flow results in higher buckling temperature and lower post-buckling deflection, i.e. results in a stiffer panel. The clamped edge boundary condition has proved to have better response than the simply supported one.

References

- [1] Xue D. Y. and Mei, C., 1993, "Finite Element Nonlinear Panel Flutter with Arbitrary Temperatures in Supersonic Flow", *AIAA Journal*, 31 (1), pp. 154-162.
- [2] Joradan P. F., 1956, "The Physical Nature of Panel Flutter", *Aero Digest*, pp. 34-38.
- [3] Tawfik M., Ro, J. J., and Mei, C., 2002, "Thermal Post-Buckling and Aeroelastic Behavior of Shape Memory Alloy Reinforced Plates", *Smart Materials and Structures*, 11, pp. 297-307.
- [4] Dowell E. H., 1970, "A Review of the Aeroelastic Stability of Plates and Shells", *AIAA Journal*, 8 (3), pp. 385-399.
- [5] Ashly, H. and Zartarian, G., 1956, "Piston Theory - A New Aerodynamic Tool for Aeroelastician", *Journal of Aeronautical Science*, 23, pp. 1109-1118.
- [6] Mei C., Abdel-Motagaly, K., and Chen, R., 1999, "Review of nonlinear panel flutter at supersonic and hypersonic speeds", *Appl. Mech. Rev.*, 52 (10), pp. 321-332.
- [7] Liaw, D. G., 1997, "Nonlinear Supersonic Flutter of Laminated Composite Plates under Thermal Loads", *Computers & Structures*, 65 (5), pp. 733-740.
- [8] Abdel-Motagaly, K., Chen, R., and Mei, C., 1999, "Effects of Flow Angularity on Nonlinear Supersonic Flutter of Composite Panels Using Finite Element Method", 40th Structure, Structural Dyn. and Mat. Conf., St louis MO, pp. 1963-1972.
- [9] Mei, C., 1977, "A Finite-Element Approach for Nonlinear Panel Flutter", *AIAA Journal*, 15 (8), pp. 1107-1110.
- [10] Dixon, I. R. and Mei, C., 1993, "Finite Element Analysis of Large-Amplitude Panel Flutter of Thin Laminates", *AIAA Journal*, 31 (4), pp. 701-707.
- [11] Sarma, B. S. and Varadan, T. K., 1987, "Nonlinear Panel Flutter By Finite Element Method", *AIAA Journal*, 26 (5), pp. 566-574.
- [12] Dongi, F., Dinkler, D., and Kroplin, B., 1996, "Active Panel Flutter Suppression Using Self-Sensing Piezoactuators", *AIAA Journal*, 34 (6), pp. 1224-1230.
- [13] Lee, I., Jin, H., and Oh, H-Kwon, 2003, "Aerothermoelastic Phenomena of Aerospace and Composite Structures", *Journal of Thermal Stresses*, 23, pp. 525-546.
- [14] Dai, K. Y., Liu, G. R., Han, X., Lim, K. M., 2005, "Thermomechanical Analysis of Functionally Graded Material (FGM) Plates Using Element-Free Galerkin Method". *Computers & Structures*, 83, pp. 1487-1502.
- [15] Birman, V., 1997, "Stability of Functionally Graded Shape Memory Alloy Sandwich Panels". *Journal of Smart Material and Structure*, 6, pp. 278-286.
- [16] El-Abbasi, N., Meguid, S. A., 2000, "Finite Element Modeling of the Thermoelastic Behavior of Functionally Graded Plates and Shells". *International Journal of Computational Engineering Science*, 1 (1), pp. 151-165.
- [17] Reddy, J. N., 2000, "Analysis of Functionally Graded Plates". *International Journal for Numerical Methods in Engineering*, 47, pp. 663-684.

- [18] He, X.Q., Ng, T. Y., Sivashanker, S., Liew, K. M., 2001, "Active Control of FGM Plates with Integrated Piezoelectric Sensors and Actuators". *International Journal of Solids and Structures*, 38, pp. 1641-1655.
- [19] Javaheri, R., Eslami, M. R., 2002, "Thermal Buckling of Functionally Graded Plates Based on Higher Order Theory". *Journal of Thermal Stresses*, 25, pp. 603-625.
- [20] Woo, J., Meguid, S. A., Liew, K. M., 2003, "Thermomechanical Post-buckling Analysis of Functionally Graded Plates and Shallow Cylindrical Shells". *Acta Mechanica*, 165, pp. 99-115.
- [21] Yang, J., Kitipornchai, Liew, K. M., 2004, "Non-Linear Analysis of the Thermo-Electro-Mechanical Behavior of Shear Deformable FGM Plates With Piezoelectric Actuators". *International Journal for Numerical Methods in Engineering*, 59, pp. 1605-1632.
- [22] Zenkour, A. M., 2005, "Generalized Shear Deformation Theory for Bending Analysis of Functionally Graded Plates". *Journal of Applied Mathematical Modeling*, 30, pp. 67-84.
- [23] Kim, Y. W., 2005, "Temperature Dependent Vibration Analysis of Functionally Graded Rectangular Plates". *Journal of Sound and Vibration*, 284, pp. 531-549.
- [24] Batra, R. C., Jin, J., 2005, "Natural Frequencies of A Functionally Graded Anisotropic Rectangular Plate". *Journal of Sound and Vibration*, 282, pp. 509-516.
- [25] Qian, L. F., Batra, R. C., 2005, "Design of Bidirectional Functionally Graded Plate for Optimal Natural Frequencies". *Journal of Sound and Vibration*, 280, pp. 415-424.
- [26] Tauchart, T. R., 1991, "Thermally Induced Flexure, Buckling, and Vibration of Plates", *Appl. Mech. Rev.*, 44 (8).
- [27] Gray, C. C., Mei, C., 1991, "Finite Element Analysis of Thermal Post-Buckling and Vibrations of Thermally Buckled Composite Plates", *AIAA Journal*, 1239-CP, pp. 2996-3007.
- [28] Thornton, E. A., 1993 "Thermal Buckling Of Plates And Shells", *Appl. Mech. Rev.*, 46 (10), pp. 485-506.
- [29] Parakash, T. and Ganapathi, M., 2004, "Supersonic Flutter Characteristics Of Functionally Graded Flat Panels Including Thermal Effects", *Journal of Composite Structures*, 72, pp. 10-18.
- [30] Touloukian, Y. S., 1967 "Thermophysical Properties of High Temperature Solid Materials", McMillan, New York.